SLAC-PUB-4808
December 1988
(A)

Damping Ring Designs for a TeV Linear Collider*

T. O. RAUBENHEIMER, L. Z. RIVKIN, R. D. RUTH
Stanford Linear Accelerator Center, Stanford University, Stanford, California 94309

ABSTRACT

In this paper we present a damping ring design for the TLC (TeV Linear Collider). The ring operates at 1.8 GeV. It has normalized emittances of $\gamma\epsilon_x = 2.8\,\mu$mrad and $\gamma\epsilon_y = 25.4$ nmrad. The damping times are $\tau_x = 2.5$ ms and $\tau_y = 4.0$ ms. To achieve these extremely low emittances and fast damping times, the ring contains 22 m of wigglers.

1. INTRODUCTION

In this paper we discuss a damping ring for the TLC, a TeV linear collider.[1)] The basic design goals of the TLC damping ring are compared with those of the Stanford Linear Collider (SLC) damping rings in Table 1. The normalized horizontal emittance of the TLC ring is an order of magnitude smaller than that of the SLC ring, and the desired repetition rate has increased by a factor of two. Furthermore, the TLC ring needs to achieve an emittance ratio of 100:1. Thus the vertical emittance must be damped to a value three orders of magnitude smaller than the SLC emittance. This implies that TLC ring will either have much faster damping times than the SLC ring or be much larger, thereby damping more bunches at once.

The present design of the TLC operates in a multi-bunch mode. The linac accelerates batches of bunches, where the bunches within a batch are separated by roughly 20 cm and each bunch contains 2×10^{10} particles. To prevent multi-bunch instabilities we need to use a specially designed RF system; a discussion of multi-bunch instabilities is found in Ref. 2. In addition, we would like to operate the ring below the longitudinal microwave instability threshold. Thus, the threshold current must be 30% larger than that in the SLC ring. To achieve this without increasing the longitudinal emittance significantly, the TLC ring must have a very low impedance and a large momentum compaction.

Table 1. Basic parameters of the SLC and TLC damping rings.

	TLC	SLC
Energy	$1 \sim 2$ GeV	1.15 Gev
Emittance, $\gamma\epsilon_x$	$3.0\,\mu$mrad	$36.\,\mu$mrad [3)]
Emittance, $\gamma\epsilon_y$	30. nmrad	–
Repetition rate	360 Hz	180 Hz
Bunch length	4 mm	5 mm [4)]
Threshold Current	batches of 10 bunches of 2×10^{10}	1.5×10^{10} [4)]

In the next section we discuss the design goals. Then using simple scaling laws, we show the dependance of the various design parameters such as the lattice, main bending field, bending angle per bend, etc. This is applied to illustrate problems with the wiggler damping ring,[5)] an option that seemed promising for low emittances and fast damping times. We then discuss the effect of damping wigglers and methods of changing the damping partitions. Because the parametric dependances become complex, we use a computer program to search for a lattice which satisfies the design criteria and uses a minimal length of wigglers.

In Sec. 3 we present a design which meets all of the specified requirements. We discuss the various portions of the ring, the arcs, the insertion regions, and the wigglers. We then detail the chromaticity correction scheme and the resulting dynamic aperture. Finally, in Sec. 5 we discuss tolerances and methods of loosening the tolerances on alignment and on the extraction kickers.

⋆ Work supported by the Department of Energy, contract, DE – AC03 – 76SF00515

Contributed to DPF Summer Study Snowmass '88

High Energy Physics in the 1990's, Snowmass, Colorado, June 27 - July 15, 1988.

2. DESIGN CONSIDERATIONS

2.1. Basic Parameters

There are two main parameters we need to consider when designing a damping ring: the ring's emittance and the damping times. The emittance of an extracted beam is

$$\epsilon = \epsilon_i e^{-2t/\tau} + (1 - e^{-2t/\tau})\epsilon_{\rm ring} \ , \qquad (2.1)$$

where ϵ_i is the emittance of the injected beam and $\epsilon_{\rm ring}$ is the ring emittance including the effects of intrabeam scattering. Here, τ is the horizontal or vertical damping time, and t is the time the bunch is in the ring. The present TLC design requires that the extracted beam have normalized emittances of $\gamma\epsilon_x \leq 3 \times 10^{-6}$ and $\gamma\epsilon_y \leq 3 \times 10^{-8}$. We assume an injected beam emittance of $\gamma\epsilon_i = 3 \times 10^{-3}$, which is realistic for a positron beam and an order of magnitude too large for an electron beam. Thus the vertical emittance needs to be decreased by five orders of magnitude. Damping the bunch for seven vertical damping times will reduce the first term of Eq. (2.1) by six orders of magnitude. The limit on the vertical emittance of the ring is then

$$\gamma\epsilon_{y\,\rm ring} \leq 2.7 \times 10^{-8}\,{\rm mrad} \ . \qquad (2.2)$$

In a storage ring built in the horizontal plane the vertical emittance is mainly determined by the coupling between the horizontal and vertical planes. Intrabeam scattering, which increases the horizontal emittance, has a very small effect on the vertical.[6,7] We will discuss the tolerances necessary to achieve the limit — Eq. (2.2) — in Sec. 5.

The required damping times are determined from the desired repetition rate (360 Hz) the number of damping times per bunch (7) and the number of batches stored in the ring at once (N_b)

$$\tau_x, \tau_y \leq \frac{1}{f_{\rm rep}} \frac{N_b}{\#\ \text{of damping times}} = N_b 0.397\,{\rm ms} \ . \qquad (2.3)$$

The maximum number of batches stored in the ring is limited by the kickers needed for injection/extraction. We assume that the time for the kickers to turn on, extract/inject a batch, and turn off is less than 100 ns.[8] Thus the batches must be separated by at least 50 ns. Since the number of batches is roughly proportional to the size of the ring we can define an effective damping time as

$$\tau_{\rm eff} \equiv \tau \frac{50\,{\rm ns}}{T_0} \leq 0.397\,{\rm ms} \ , \qquad (2.4)$$

where T_0 is the revolution time of the ring.

For reasons we will discuss later, it is desirable that the horizontal damping time be less than or equal to the vertical; thus only the vertical damping time is limited by Eq. (2.3). Furthermore, assuming that $\tau_x \lesssim \tau_y$, the horizontal emittance of the extracted beam is very nearly equal to the horizontal emittance of the ring. Thus

$$\gamma\epsilon_{x\,\rm ring} \leq 3 \times 10^{-6}\,{\rm mrad} \ . \qquad (2.5)$$

Equations (2.4) and (2.5) determine the basic parameters. Initially, to study these parameters, we make the assumption that all the bending magnets are the same and we ignore the effect of intrabeam scattering. Now we can write simple expressions for $\gamma\epsilon_{x0}$ and $\tau_{y\,\rm eff}$,[9] the two quantities we want to minimize:

$$\tau_{y\,\rm eff} = 8.47 \times 10^6 \frac{\rho_B f_w}{J_y \gamma^3} \qquad (2.6)$$

$$\gamma\epsilon_{x0} = 3.84 \times 10^{-13} \frac{\gamma^3}{J_x} \frac{\langle\mathcal{H}\rangle_{\rm mag}}{\rho_B} \ . \qquad (2.7)$$

Here, ρ_B is the *local* bending radius of the bend magnets and $\langle\mathcal{H}\rangle_{\rm mag}$ is the Courant–Snyder dispersion invariant which equals the average of $\mathcal{H} \equiv \gamma\eta_x^2 + 2\alpha\eta_x\eta_x' + \beta\eta_x'^2$ over the bending magnets. Also, $J_{x,y}$ is the horizontal (vertical) damping partition number, and f_w is equal to ρ_B divided by the average bending radius in the bending magnets, ρ_0. Note that with normal bends $f_w = 1$, but in a wiggler ring[5] where the bending magnets bend in both directions, $f_w < 1$.

The emittance of a ring can be reduced by reducing the dispersion in the bend magnets, reducing the strength of the bends, or decreasing the energy of the ring. Unfortunately, the damping times are *increased* by reducing the bend magnet strength or decreasing the energy of the ring. This implies that the dispersion in the bends is the only free parameter. Unfortunately, it is constrained by the longitudinal microwave instability which increases the longitudinal emittance.

At this point it is worth discussing three additional parameters which constrain the design: (1) the longitudinal microwave instability which was just mentioned, (2) the dynamic aperture, and (3) the energy of the ring. The microwave instability, also called turbulent bunch lengthening, occurs at a given current when the longitudinal impedance is larger than a threshold, denoted $(Z/n)_t$. We want to keep this threshold as large as possible to avoid bunch lengthening and longitudinal instabilities. It can be estimated as

$$(Z/n)_t \approx \frac{(2\pi)^{3/2} E \sigma_\epsilon^2 \sigma_z \alpha}{N e^2 c} \mathcal{F} \ , \qquad (2.8)$$

where E is the energy, σ_ϵ is the relative energy spread, and σ_z is the bunch length. In addition, α is the momentum compaction, N is the number of e^+/e^- per bunch, and e and c are the electron charge and the speed of light. Finally, $\mathcal{F}$ is a form factor which is greater than 1.[10] At the 1987

ICFA workshop on Low Emittance Beams,[11] an impedance of

$$Z/n \geq 0.2\,\Omega \tag{2.9}$$

was determined to be the minimum reasonable, physically attainable value.

Next we should consider the dynamic aperture. The dynamic aperture of the ring is a function of the sextupoles needed to correct the chromaticity. To prevent particle losses the dynamic aperture should be many times the *injected* beam size. Unfortunately, rings with small emittances tend to have high tunes and large uncorrected chromaticities. This makes the desired dynamic aperture difficult to achieve. Thus we would like to choose a lattice which naturally has a large dynamic aperture.

Finally, the other parameter we mentioned is the ring energy which we would prefer to have low. There are three primary reasons for this: (1) it makes the magnets cheaper, (2) it keeps the longitudinal emittance small, and (3) it makes bunch compression easier. The TLC requires that the damping ring bunch be compressed longitudinally by, roughly, a factor of 100. Since one does not want an uncorrelated energy spread much greater than 1% in the linac, we need to perform at least a portion of the bunch compression at an energy 10 times that of the damping ring.[12] Unfortunately, at higher energies it becomes more difficult to perform the compression without degrading the beam emittances.

2.2. Scaling

Now we can combine these expressions to determine the dependencies of the parameters. Using the definition of and maximum value for $\tau_{y\,\mathrm{eff}}$ — Eqs. (2.6) and (2.4) — we find an expression for the energy of the ring as a function of the bending field and f_w:

$$B_0(KG)\gamma^2 = f_w \frac{1.44 \times 10^5}{\tau_{y\,\mathrm{eff}}} . \tag{2.10}$$

In this equation, J_y is assumed to be equal to 1, since it cannot be changed without introducing vertical dispersion which would degrade the vertical emittance. Note that for our parameters, a normal ring, with saturated bending magnets (20 KG), must operate at 2.2 GeV to meet the damping time requirements.

In a similar manner, using Eqs. (2.7) and (2.10), we find an equation for the emittance as a function of f_w, $\langle\mathcal{H}\rangle_{\mathrm{mag}}$, and J_x:

$$\gamma\epsilon_{x0} = \frac{3.25 \times 10^{-6}}{\tau_{y\,\mathrm{eff}}} \frac{\langle\mathcal{H}\rangle_{\mathrm{mag}} f_w}{J_x} . \tag{2.11}$$

Next we use Eq. (2.10), along with an equation for the relative energy spread in the ring:[9]

$$\sigma_\epsilon^2 = \frac{C_q\gamma^2}{J_\epsilon \rho_B} = 2.25 \times 10^{-11} \frac{\gamma B(KG)}{J_\epsilon} , \tag{2.12}$$

to re-write the expression for $(Z/n)_t$ (Eq. (2.8))

$$(Z/n)_t \approx \mathcal{F}\frac{5.43 \times 10^{11}}{N} \frac{\sigma_z}{\tau_{y\,\mathrm{eff}}} \frac{\alpha f_w}{J_\epsilon} . \tag{2.13}$$

Notice that the energy no longer appears in Eqs. (2.11) and (2.13). It is determined by the main bending field and the desired damping time, $\tau_{y\,\mathrm{eff}}$ (Eq. (2.10)).

In Eq. (2.13) we have ignored the constraints on the energy spread. A large energy spread reduces the lifetime and increases the longitudinal emittance. In practice we are limited to a relative energy spread of a couple tenths of a percent and thus there is a lower bound on α. Using $(Z/n)_t = 0.2\,\Omega$, this bound is:

$$\alpha \geq 1.19 \times 10^{-18} \frac{N}{\mathcal{F}\gamma\sigma_\epsilon^2\sigma_z} . \tag{2.14}$$

Notice that the bound is inversely proportional to the energy, implying that a higher energy is desirable. In contrast, the energy does not appear in Eq. (2.13) where the energy spread is a free parameter. In most cases, we will find that we cannot increase the energy spread sufficiently to gain from the $1/\gamma$ dependance of Eq. (2.14).

If we assume that $\sigma_z \approx 4\,\mathrm{mm}$, we see that given an effective damping time, we only have six quantities: J_x, J_ϵ, f_w, B, $\langle\mathcal{H}\rangle_{\mathrm{mag}}$, and α, which can be varied to fit the requirements on the energy, the emittance, and the longitudinal impedance threshold. Unfortunately, the system is more tightly constrained since the six variable parameters are not independent.

The bending field, B_0, is determined by the energy and f_w. We are then left with fitting the emittance and the impedance threshold, one of which we would like small and the other large. The parameter f_w can be removed by considering the ratio $(Z/n)_t/\gamma\epsilon_{x0}$. To optimize this ratio, *i.e.* make it large, we can increase J_x at the expense of J_ϵ and/or increase the ratio $\alpha/\langle\mathcal{H}\rangle_{\mathrm{mag}}$. The easier option is that of changing the damping partition numbers. They can be changed by using combined function bending magnets or a Robinson wiggler.[13,14] Unfortunately, we do not wish to increase J_x much beyond 2. Thus, we also have to consider maximizing the ratio of $\alpha/\langle\mathcal{H}\rangle_{\mathrm{mag}}$.

For a given lattice design, we can write down some approximate scaling laws. In most lattices, assuming that the phase advance per cell is held constant, $\langle\mathcal{H}\rangle_{\mathrm{bend}} \propto \Theta^3\rho_{\mathrm{ave}} \propto \Theta^2 L_{cell}$ and $\alpha \propto \Theta^2$. Thus the ratio of $\alpha/\langle\mathcal{H}\rangle_{\mathrm{bend}}$ is inversely proportional to the length of the cell. Notice that unlike normal scaling laws for damping rings, the bend angle is not at our disposal for minimizing the emittance; it is determined by $(Z/n)_t$.

2.3. Lattices

In choosing a lattice we want one that naturally has a large dynamic aperture and a large ratio of $\alpha/\langle\mathcal{H}\rangle_{\rm mag}$. The three lattices that seem best suited to our requirements are the FODO lattice, the triple bending achromat (TBA) lattice proposed by Vignola,[15] and the TME lattice described by Steenbergen.[16] Wiedemann has compared the double focusing achromat (DFA) and triplet achromat lattices with the FODO lattice.[17] He found that the FODO lattice had significantly better chromatic properties than the other two.

The TBA lattice has been studied by Bisognano[18] with application to a 750 MeV storage ring for FEL's and by Jackson[19] for a 1–2 GeV synchrotron light source. It has the advantage of probably being less expensive to construct than a FODO structure since fewer cells are needed to achieve the same emittance. In addition, the lattice, potentially, has a larger ratio of $\alpha/\langle\mathcal{H}\rangle_{\rm mag}$. Unfortunately, the lattices proposed to date have $\alpha/\langle\mathcal{H}\rangle_{\rm mag}$ ratios that are an order of magnitude too small.

The TME lattice would also be cheaper to build than a FODO lattice and it should be investigated further. In addition, another lattice worth examining would be an extreme version of the FODO lattice where combined function bends completely replace the defocusing quadrupoles. This would be the most compact and could offer the best ratio of $\alpha/\langle\mathcal{H}\rangle_{\rm mag}$. Unfortunately, it may not be feasible to achieve the necessary gradients in the bends.

For our initial design we chose to use a FODO lattice. This choice was based mostly upon the superior dynamic aperture characteristics of the lattice. Another advantage of the FODO lattice is that it allows for local chromatic correction, *i.e.* placing the correcting sextupoles next to the quadrupoles which generate the chromaticity. This results in looser tolerances on the vertical orbit; see the discussion in Sec. 5.

While we can create a simple FODO design on paper that would satisfy the requirements, the necessary magnetic fields make it technically unfeasible. The problems arise because extremely strong magnetic fields are needed in the quadrupoles to keep the cell length short. This leaves us the option of: (1) using combined function bends to minimize the cell length, (2) varying J_x and J_ϵ, and (3) possibly using wigglers to decrease the required main bending field and increase the energy spread. Before discussing the use of separate wigglers, we feel it is useful to quickly discuss the wiggler ring option.

2.4. Wiggler Ring

The wiggler ring design has excellent damping times at low energies. It achieves this, as wigglers do, by bending the particle a lot while generating very little dispersion. Since the damping times can be much shorter than a conventional ring, the wiggler ring can operate at lower energies and thus achieve the necessary low emittances. Unfortunately, the $(Z/n)_t$ of a wiggler lattice is lower than that of a comparable conventional ring. To understand this we have to compare $\langle\mathcal{H}\rangle_{\rm bend}$ and α in the two designs.

$\mathcal{H}$ can be written as the sum of two squares: $\mathcal{H} = \eta_x^2/\beta + (\eta_x\alpha + \eta_x'\beta)^2/\beta$. Since the second term depends upon η_x' which does not contribute to α, we would like to keep it small. The wiggler magnet bends in both the positive and negative x direction, and thus η_x and η_x' will oscillate. This will force the second term in $\langle\mathcal{H}\rangle_{\rm bend}$ to be larger. One could minimize the effects of the oscillations by making the wiggler period shorter, but one runs into technical limitations quickly. Another problem is that the length of the cells in the wiggler ring will be longer than in a normal ring. Using the scaling laws discussed at the end of Sec. 2.2, we can see that this increases $\langle\mathcal{H}\rangle_{\rm mag}$ without increasing α.

Before concluding this section, we note that many wiggler ring designs were presented at the 1987 ICFA workshop.[11] Unfortunately, these all had very long bunch lengths ($\sigma_z > 15\,$mm). The long bunch lengths are necessary to meet the impedance limitations and to reduce the effect of intrabeam scattering. However, if the $(Z/n)_t$ is not an issue or if the bunch length is allowed to be longer, the wiggler ring is an attractive option.

2.5. Damping Wigglers

As was mentioned in Sec. 2.2, it is very hard to build a conventional or wiggler ring which meets all of the design criteria. This leads us to consider the effects of including separate damping wigglers in regions of zero dispersion. By locating the wigglers in regions of zero dispersion, $\langle\mathcal{H}\rangle_{\rm mag}$ in the wigglers will be small, and thus one can significantly reduce both the damping times and the emittance. In addition, damping wigglers increase the energy spread in the ring. Thus, despite the slight decrease in α resulting from the increased length of the ring, damping wigglers can significantly improve the ratio of $(Z/n)_t/\gamma\epsilon_{x0}$.

The scaling formulas Eq. (2.10) thru (2.13) can be modified to include the effects of damping wigglers:

$$B_0(KG)\gamma^2(1+F_w) = \frac{1.44\times10^5}{\tau_{y\,\rm eff}} \tag{2.15}$$

$$\gamma\epsilon_{x0} = \frac{3.25\times10^{-6}}{\tau_{y\,\rm eff}J_x}\frac{\left(\langle\mathcal{H}\rangle_{\rm bend} + 6\overline{\beta_x}F_w\rho_0/5\pi k_w^2\rho_w^3\right)}{(1+F_w)^2} \tag{2.16}$$

$$(Z/n)_t \approx \mathcal{F}\frac{5.43\times10^{11}}{N\tau_{y\,\rm eff}}\frac{\sigma_z\alpha}{J_\epsilon}\frac{\left(1+8F_w\rho_0/3\pi\rho_w\right)}{(1+F_w)^2}\ , \tag{2.17}$$

where the parameter F_w is a measure of the effectiveness of the wigglers,

$$F_w \equiv L_w\rho_0/4\pi\rho_w^2\ . \tag{2.18}$$

Here, L_w and B_w are the length and peak field of the wiggler; $\overline{\beta_x}$ is the average beta function in the wiggler, and k_w

is the wiggler wave number, $k_w = 2\pi/\lambda_w$ where λ_w is the wiggler period. Also, ρ_0 and ρ_w are the bending radii of the main bends and the wiggler. Both bending radii are proportional to the energy over the respective magnetic fields. We have assumed sinusoidal wigglers, and thus the integral of $B_w^2(s)$ over the wiggler is equal to $1/2B_w^2$. In addition, we assume that $\overline{\beta_x} \gg \lambda_w/2\pi$ so that the $\eta_x'^2\beta_x$ term dominates in $\langle\mathcal{H}\rangle_{\text{wig}}$. We do not consider decreasing $\overline{\beta_x}$ significantly since that would increase the chromaticity of the ring and might decrease the dynamic aperture.

Looking at Eqs. (2.15) thru (2.17), we can see that the largest effect occurs when $\rho_0 \gg \rho_w$ and F_w is large, *i.e.* when $B_0 \ll B_w$. Unfortunately, we are limited when increasing B_w since the η_x' created by the wigglers will blowup the emittance. This constrains the period of the wiggler and can be expressed

$$B_w^3\overline{\beta_x}\lambda_w^2\frac{F_w}{(1+F_w)} \ll 1.33\times10^9\gamma\epsilon_{x0}J_x\ . \qquad (2.19)$$

We consider two cases, relatively long Nd-Fe-B hybrid wigglers and short superconducting wigglers. In the Nd-Fe-B hybrid wigglers the maximum field can be specified as a function of the gap and the period[20]

$$B_w \le 3.44\exp\left[-\frac{g}{\lambda_w}\left(5.08-1.54\frac{g}{\lambda_w}\right)\right]\ , \qquad (2.20)$$

for $0.08 < g/\lambda_w < 0.7$. To achieve a field of $B_w = 22$ KG with a gap of 2 cm, λ_w must be at least 20 cm. This is much less than the limit imposed by Eq. (2.19); with $\overline{\beta_x} \approx 4$ m, Eq. (2.19) limits $\lambda_w \ll 35$ cm. In the superconducting case we use a 40 KG field and a 20 cm period. This is (arbitrarily) scaled from the 50 KG superconducting wiggler in the DCI ring at LURE[21] with a 65 mm gap and 26 cm period. Assuming that $\overline{\beta_x} \approx 1$ m since the wigglers are shorter, the 20 cm period is less than the limit specified by Eq. (2.19): $\lambda_w \ll 29$ cm.

If we assume that the condition Eq. (2.19) is met, we can use the simple scaling for $\langle\mathcal{H}\rangle_{\text{bend}}$ and α, discussed earlier in Sec. 2.2, to express $\gamma\epsilon_{x0}$ and $(Z/n)_t$:

$$\begin{aligned}\gamma\epsilon_{x0} &\propto \frac{\Theta^2 L_{cell}}{J_x(1+F_w)^2}\\ (Z/n)_t &\propto \frac{\Theta^2}{J_\epsilon(1+F_w)^2}\frac{(1+8F_w\rho_0/3\pi\rho_w)}{1+L_{\text{wig}}/L_{\text{ring}}}\ ,\end{aligned} \qquad (2.21)$$

where L_{wig} is the length of the wigglers and the associated insertion regions and L_{ring} is the total length of the ring. We would like to keep the wiggler lengths short, and thus it is desirable to maximize the wiggler fields and minimize the bending field. While decreasing the main bending field increases the cell length, it still decreases the emittance without decreasing the impedance threshold. Unfortunately, decreasing the main bending field and the length of the wigglers forces us to higher energies.

Because the additional parameters make the analysis complex, a simple computer program was written that calculates $\gamma\epsilon_{x0}$ and $(Z/n)_t$. It uses Eqs. (2.15) thru (2.17) and the relations for $\langle\mathcal{H}\rangle_{\text{bend}}$ and α in FODO cells[22] for the calculation. We chose phase advances per cell of $\nu_x = 0.3$ and $\nu_y = 0.1$; while these phase advances do not minimize the emittance, they are chosen to be regions where the chromaticity does not increase rapidly. The cell lengths are calculated by adding the length of two bending magnets to 0.8 m, length for the drifts and quadrupoles. We then calculate the ring length from the number of cells required plus three times the length of wigglers required, allowing space for dispersion suppression, quadrupole doublets, etc. in the insertion. We use the wiggler parameters: $B_w = 22$ KG, $\lambda_w = 20$ cm, $\overline{\beta_x} = 4$ m and $B_w = 40$ KG, $\lambda_w = 20$ cm, $\overline{\beta_x} = 1$ m, and solve for solutions with $\gamma\epsilon_{x0} = 2.0\times10^{-6}$ and $(Z/n)_t = 0.2\,\Omega$; the value of $\gamma\epsilon_{x0}$ was chosen to allow for the increase in emittance due to intrabeam scattering. Finally, since wigglers are expensive, we attempt to minimize the length included. Tables 2 and 3 list our solutions with the shortest wigglers for three energies.

Notice that the solutions for the superconducting case in Table 3 have a higher main bending field and smaller bending angles than those in Table 2. This occurs because the stronger wigglers cause a larger energy spread, lowering the momentum compaction required to meet the impedance threshold $(Z/n)_t = 0.2\,\Omega$. Thus one can decrease the bending angle per bend, increase the main bending field and decrease the length of the wigglers, see Eq. (2.21). Since we feel that the wigglers calculated are too expensive, and we do not wish to go much higher in energy, we need to also consider changing the damping partitions. This will further increase the energy spread and lower the emittance, allowing us to increase the main bending field and thereby decrease the length of the wigglers.

Table 2. Solutions for a FODO lattice with 22 KG wigglers: $\gamma\epsilon_{x0} = 2.0\times10^{-6}, (Z/n)_t = 0.2\,\Omega$.

Energy	# of cells	B_0	L_w	L_{ring}
1.75 GeV	58	5.0 KG	39 m	210 m
2.0 GeV	70	4.5 KG	33 m	225 m
2.25 GeV	80	4.0 KG	28 m	250 m

Table 3. Solutions for a FODO lattice with 40 KG wigglers: $\gamma\epsilon_{x0} = 2.0\times10^{-6}, (Z/n)_t = 0.2\,\Omega$.

Energy	# of cells	B_0	L_w	L_{ring}
1.75 GeV	90	8 KG	11 m	142 m
2.0 GeV	102	6.5 KG	9 m	170 m
2.25 GeV	112	6.0 KG	7.5 m	185 m

2.6. DAMPING PARTITIONS

The damping partitions describe the relative rates of the horizontal, vertical and longitudinal damping. Since the injected longitudinal emittance is usually much closer to the damped value than is the horizontal or vertical, it is reasonable to increase the horizontal and/or vertical partitions at the expense of the longitudinal. As was mentioned earlier the vertical partition is effectively fixed, but we can increase the horizontal damping partition and thereby lower the horizontal emittance. In addition, decreasing the longitudinal damping partition increases the energy spread, and thereby $(Z/n)_t$.

The damping partitions in a ring can be changed by using combined function bending magnets or Robinson wigglers.[13] The partitions can be written:[9]

$$J_x = 1 + \frac{\oint \eta_x/\rho(1/\rho^2 + 2K_1)ds}{\oint ds/\rho^2} \qquad J_\epsilon = 3 - J_x \ , \quad (2.22)$$

where K_1 is negative for a horizontally focusing quadrupole field.

In the case of a Robinson wiggler, Eq. (2.22) becomes

$$J_x = 1 + \frac{\overline{\eta_x} L_{\rm Rob} K_1}{2\pi(1+F_w)} \frac{\rho_0}{\rho_{\rm Rob}} \ , \qquad (2.23)$$

where $L_{\rm Rob}$ and $\rho_{\rm Rob}$ are the length and bending radius of the Robinson wiggler. Thus we see that we would like to place it in a region of high dispersion. Unfortunately, this causes the emittance to increase. The emittance blowup is

$$\Delta\gamma\epsilon_x = \frac{3.25\times10^{-6}}{\tau_{y\,\rm eff}} \frac{1}{J_x(1+F_w)^2} \frac{L_{\rm Rob}}{4\pi^2} \frac{\overline{\eta_x}^2}{\overline{\beta_x}} \frac{\rho_0^2}{\rho_{\rm Rob}^3} \ . \quad (2.24)$$

To keep the emittance increase small, the wiggler should be built so both $\rho_{\rm Rob}$ and $|K_1|$ are large and it should be placed in a region where β_x is large also. For example with the parameters: $\eta_x = 20\,$cm, $\beta_x = 10$ m, $\rho_0 = 5$ m, and $K_1 = 17\,\rm m^{-2}$, a wiggler length of 4 m will increase J_x by 1.1 and increase the emittance by less than 5%. The problems with this are: (1) extra length is required for the wiggler insertion and (2) to achieve the strong quadrupole fields the wiggler would have to be built as large aperture quadrupoles with the beam passing off-center; technically this might present a problem.

The other option, that of using combined function bends, seems to be easier. In this case Eq. (2.22) is

$$J_x = 1 + \frac{\alpha K_1 \rho_0 L_{\rm ring}}{\pi(1+F_w)} \ . \qquad (2.25)$$

Here the emittance is not increased by the combined function bends; in fact it should decrease slightly since the defocusing quadrupoles could be made smaller, increasing the filling factor. Furthermore, an additional insertion, which would decrease α, is not required.

Table 4. Solutions for a combined function FODO lattice with 22 KG wigglers. $\gamma\epsilon_{x0} = 2.0\times10^{-6}, (Z/n)_t = 0.2\,\Omega$.

Energy	# of cells	B_0	K_1	L_w	$L_{\rm ring}$
1.75 GeV	73	13.0 KG	$4.8\,\rm m^{-2}$	27 m	145 m
2.0 GeV	90	12.5 KG	$4.2\,\rm m^{-2}$	18 m	160 m
2.25 GeV	108	12.5 KG	$3.7\,\rm m^{-2}$	11 m	160 m

Table 5. Solutions for a combined function FODO lattice with 40 KG wigglers: $\gamma\epsilon_{x0} = 2.0\times10^{-6}, (Z/n)_t = 0.2\,\Omega$.

Energy	# of cells	B_0	K_1	L_w	$L_{\rm ring}$
1.75 GeV	96	15.0 KG	$3.4\,\rm m^{-2}$	7.25 m	113 m
2.0 GeV	112	14.5 KG	$3.3\,\rm m^{-2}$	4.75 m	125 m
2.25 GeV	120	14.0 KG	$3.2\,\rm m^{-2}$	2.75 m	140 m

Since this is the more promising route, we calculate $\gamma\epsilon_{x0}$ and $(Z/n)_t$ as we do in Tables 2 and 3, except we include the effect of a defocusing field on J_x. Obviously, it is desirable to have the largest defocusing field possible, consistent with limits on the energy spread. We calculate K_1 by choosing the larger of two expressions:

$$K_1 = \frac{14\,{\rm KG} - B_0}{B\rho\ 0.0125} \qquad K_1 = \frac{20\,{\rm KG} - B_0}{B\rho\ 0.025} \ . \qquad (2.26)$$

The first expression estimates the field achievable in an off-center quadrupole, assuming 14 KG pole tip fields and a beam pipe radius of 1.25 cm. The radius of the quadrupole is then the beam pipe radius plus the offset. The second expression estimates the field in a bending magnet with modified poles. We assume 20 KG maximum field with poles that extend to twice the beam pipe radius of 1.25 cm.

The results for the conventional and superconducting wigglers are listed in Tables 4 and 5. Notice that when compared to Tables 2 and 3, the number of cells has increased and the main bending field has increased. Because the main bends are stronger, the required length of wiggler has decreased by roughly a factor of two. Obviously this is desirable. Unfortunately, increasing the number of cells and increasing the bend strength means that the bends becomes very short, 13 cm for the 1.75 GeV case in Table 5. It is difficult to achieve the necessary field quality in such short bends since the end fields become significant.

We use the results from Table 4 to pick a starting point for our ring. We start with the lowest energy, conventional wiggler, design. This was chosen for the reasons mentioned previously in Sec. 2.1; namely, low energy makes the subsequent bunch compression easier and the magnets are easier to build. In addition, although the low energy design requires more wigglers, it is smaller and therefore (hopefully) cheaper; we have not attempted to optimize costs in a rigorous manner.

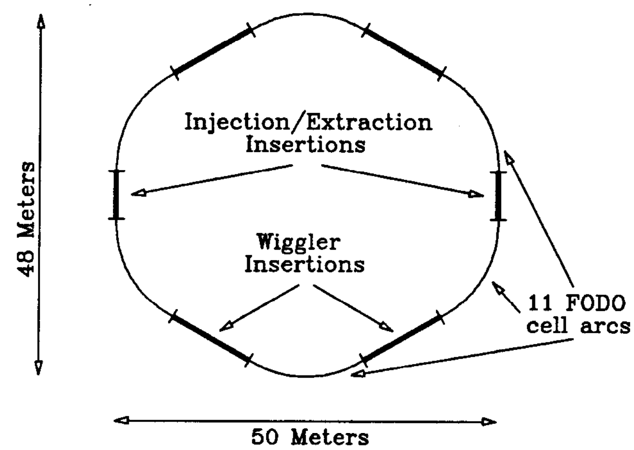

Fig. 1. Schematic of the TLC damping ring.

Table 6. TLC damping ring parameters.

Energy	$E_0 = 1.8$ GeV
Length	$L = 155.1$ m
Momentum compaction	$\alpha = 0.00120$
Tunes	$\nu_x = 24.37, \quad \nu_y = 11.27$
RF frequency	$f_{RF} = 1.4$ GHz
Current	10 batches of 10 bunches of $2 \times 10^{10} e^+/e^-$

3. BASIC LATTICE

A design for the TLC damping ring is illustrated in Fig. 1. The ring has a circumference of 155 m and operates at an energy of 1.8 GeV. There are six insertion regions, two for injection/extraction and four for wigglers. The arcs between each insertion region are composed of 11 combined function FODO cells. The ring has a superperiodicity of two. The parameters are listed in Tables 6 and 7. Table 6 lists general parameters while Table 7 lists parameters for the ring with the wigglers on and off. The optical functions β_x and β_y and the dispersion function η_x for half of the ring are plotted in Fig. 2.

The ring would operate with 10 batches of 10 bunches of 2×10^{10} electrons/positrons. The bunches in a batch are separated by 1 RF period, approximately 20 cm. Each batch is then separated by 50 ns, leaving 100 ns for the kicker pulse to rise and fall. When the wigglers are on, the normalized horizontal emittance, including the intrabeam scattering effects calculated by ZAP,[23] is 2.75×10^{-6}mrad. Because the ring operates at a relatively high energy, necessary to achieve the required damping rates, the intrabeam scattering contribution to the emittance is fairly small — about 27% of the ring emittance. The damping times are $\tau_x = 2.50$ ms and $\tau_y = 3.98$ ms. This allows each batch to remain in the ring for seven vertical damping times (vdt) when operating at a repetition rate of 360 Hz. Ignoring coupling of the horizontal and vertical planes, 7 vdt will damp a positron beam with an initial normalized emittance of 3×10^{-3} to an emittance of 2.7×10^{-9}mrad. The alignment tolerances required to achieve the 100:1 emittance ratio are discussed later in Sec. 5.

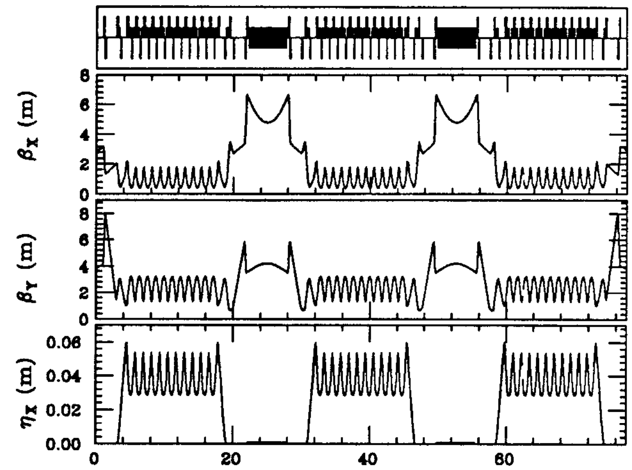

Fig. 2. Optical functions for half of the ring.

Table 7. TLC damping ring parameters.

	Wigglers Off	Wigglers On
Natural $\gamma\epsilon_x$	2.46 μmrad	2.00 μmrad
$\gamma\epsilon_x$ w/ intrabeam	3.33 μmrad	2.74 μmrad
Damping, τ_x	3.88 ms	2.50 ms
Damping, τ_y	9.19 ms	3.98 ms
Rep. rate, f_{rep}	155 Hz	360 Hz
Damp. partition, J_x	2.37	1.59
Energy spread, σ_ϵ	0.00128	0.00104
Radiation/turn, U_0	203 KeV	468 KeV
Bunch length, σ_z	5.6 mm	5.2 mm
Synch. tune, ν_s	0.0068	0.0058
$(Z/n)_t$	$\mathcal{F} \times 0.32\,\Omega$	$\mathcal{F} \times 0.20\,\Omega$
Natural chrom., ξ_x	-28.35	-28.07
Natural chrom., ξ_y	-25.10	-22.27

We wish to operate the ring below or close to the turbulent bunch lengthening threshold. The threshold is $(Z/n)_t = \mathcal{F} \times .2\,\Omega$ where $\mathcal{F}$ is a form factor greater than one.[10] While this impedance is very low (by conventional standards) we plan to achieve such a value by using a constant size beam pipe throughout the ring. The planned pipe has a 1 cm inner radius which is slightly smaller than the SLC damping rings and is approximately seven times the beam size of an injected positron beam.

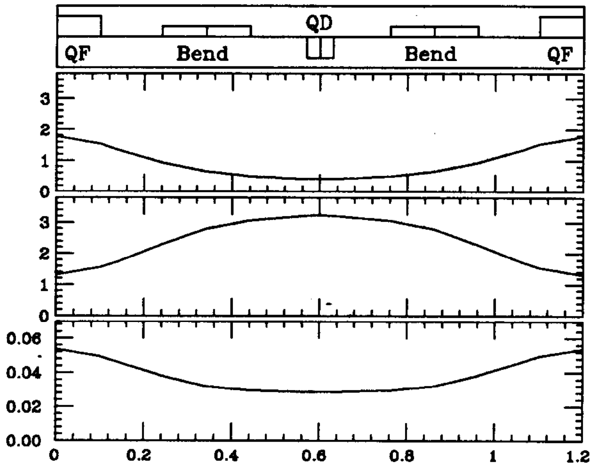

Fig. 3. Arc cell optics and magnets.

3.1. Arcs

The six arcs are constructed of 11 combined function FODO cells. The bends have an additional defocusing quadrupole gradient which re-partitions the damping. The optical functions and the magnet positions are plotted for a single cell in Fig. 3. The bend magnets bend an angle of 2.5° and have normalized defocusing gradients of $K_1 = 5.0\,\mathrm{m}^{-2}$, *i.e.* a gradient of 300 KG/meter. The QF's, the focusing quadrupoles, which are the strongest quadrupoles in the ring, have normalized gradients of $-15.7\,\mathrm{m}^{-2}$. Using a magnetic radius of $r = 1.2\,\mathrm{cm}$, 2 mm greater than the beam pipe, the QF's have pole tip fields of 11.3 KG.

This design has a little more space between magnets than the SLC damping rings do, but it is still tightly packed. There is 14 cm between the QF's and the bends and 13 cm between the bends and the QD's. Note that since the bends have large defocusing fields the QD's are very short. Since space is tight and very strong sextupoles will be needed to correct the chromaticity, we plan to use permanent magnet sextupoles similar to those successfully used in the SLC damping rings.[24)]

3.2. Injection/Extraction Insertion

The injection/extraction insertion regions have a 2 m drift space for septum magnets. On either side of the insertion drift there are additional 1.6 m drift spaces. The horizontal phase advance from the middle of the insertion drift to the center of these side drifts is approximately $\pi/2$, thus making them useful for the placement of the kicker magnets needed for injection/extraction. The optical functions for half an insertion are plotted in Fig. 4.

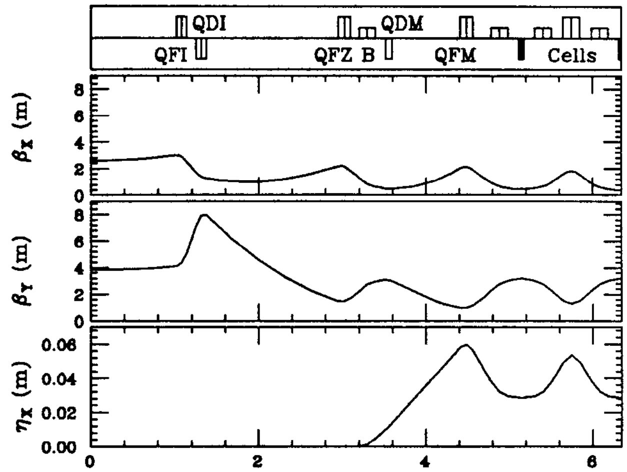

Fig. 4. Half of the injection/extraction insertion.

The dispersion is set to zero in all six of the insertion regions. This is done in the injection/extraction regions to make it easier to match the extraction transport line to the ring. Experience on the SLC has shown that properly matching the various components of the collider is crucial for obtaining small spots at the collision point. In addition, zero dispersion should make injection of the large positron beams easier.

3.3. Wiggler Insertions

The wiggler insertions are very similar to the injection/extraction insertions. Both insertions use the same dispersion suppression arrangement. The main drift in the wiggler insertion is 6 m rather than 2 m. There is also an additional quadrupole so that the wigglers can be continuously varied from full on to off while keeping the phase advance across the region constant. The lattice functions for 1/2 the insertion with the wigglers off are plotted in Fig. 5 and the same with the wigglers on is plotted in Fig. 6. Notice that the vertical focusing due to the wigglers allows β_y to have negative curvature across the insertion.

3.4. Wigglers

Wigglers are required to reduce the damping times by a factor of approximately 2.5. Thus, high peak fields are needed. Unfortunately, to prevent the wigglers from blowing up the emittance, short wiggler periods are also necessary. We chose a wiggler with a 24 KG peak field and a period of 20 cm. With this short period the wigglers actually lower the emittance. The wiggler contribution to the emittance is dominated by the η_x' generated by in the wigglers. Since β_x is approximately 4 m in the wiggler, the dispersion in the wiggler would have to be roughly 15 cm before its contribution to the emittance is comparable. We could have lowered β_x in the wiggler, but this would increase the chromaticity and likely decrease the dynamic aperture because stronger sextupoles would be needed for chromatic correction.

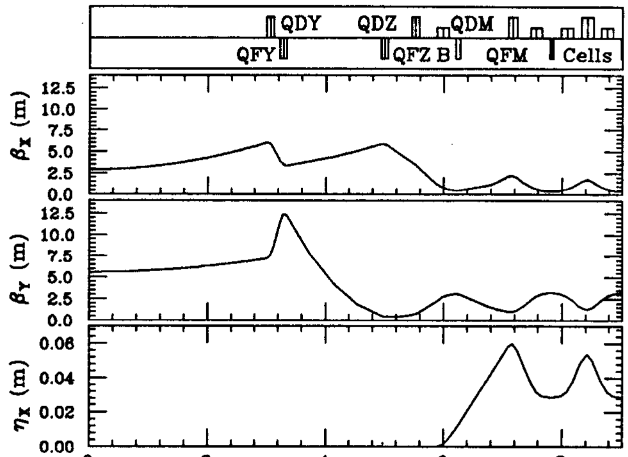

Fig. 5. Half of the wiggler insertion with wigglers off.

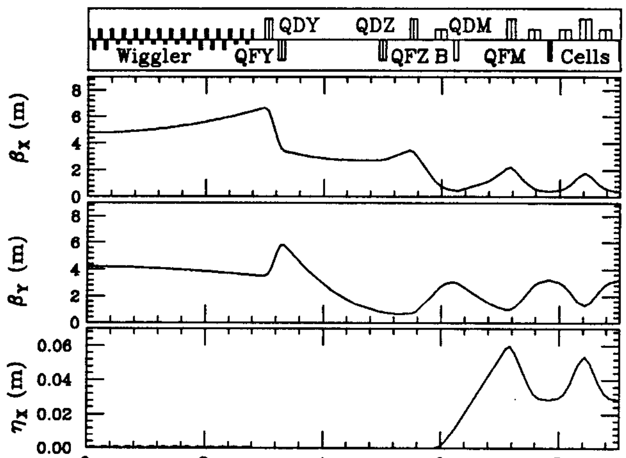

Fig. 6. Half of the wiggler insertion with wigglers on.

The period and the peak field were chosen to be within 15%[25] of the limits for Nd-Fe-B hybrid wigglers as specified in Ref. 20. If such a high peak field is not feasible, we can increase the energy of the design to 1.9 GeV and decrease the peak wiggler fields to 21 KG, the maximum field specified in this reference. The vertical damping time remains 3.98 ms and the natural horizontal normalized emittance increases to 2.29×10^{-6}mrad; intrabeam scattering further increases this to 2.85×10^{-6}mrad. The small increase in emittance occurs because the horizontal damping partition J_x increases as the wiggler gets weaker, see Eq. (2.25).

The wigglers are 5.6 m long, leaving 20 cm between the wiggler and the insertion quadrupoles. We modelled them in the lattice using hard-edged rectangular bends with the same peak field, 24 KG. The poles are 1/4 of a period long and the drifts separating the poles are also a 1/4 period long. Thus the model wigglers generate the same amount of synchrotron radiation as sinusoidal wigglers would, but the vertical focusing contribution is incorrect. With this model we should be over-estimating the vertical focusing and the four quadrupoles in the wiggler insertions should be able to easily compensate the weaker focusing.

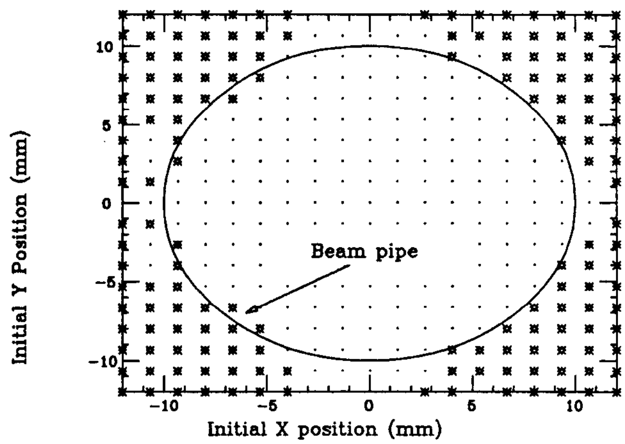

Fig. 7. Dynamic aperture for the chromatically corrected ring.

4. CHROMATIC CORRECTION

Before attempting to optimize the ring, we need to demonstrate that the chromatically corrected ring can have reasonable dynamic aperture. We currently correct the chromaticity with only two families of sextupoles located in the arcs. The integrated sextupole strengths are: $K_{2\,\mathrm{SF}} = -52.0\,\mathrm{m}^{-2}$ and $K_{2\,\mathrm{SD}} = 68.7\,\mathrm{m}^{-2}$.

The phase advance of the cells is adjusted to cancel most of the first order geometrics over an arc, 11 cells. The amplitudes of the first order geometric perturbations are proportional to:[26]

$$\begin{gathered}\int_{\mathrm{arc}} ds\beta_x^{3/2} K_2 (e^{i3\psi_x} + e^{i\psi_x} + CC) \\ \int_{\mathrm{arc}} ds\beta_x^{1/2}\beta_y K_2 (e^{i\psi_x + 2\psi_y} + e^{i\psi_x} + e^{i\psi_x - 2\psi_y} + CC)\end{gathered} \tag{4.1}$$

where CC represents the complex conjugate. Since the cells are periodic, these integrals can be minimized by making the arc phase advances integral multiples of 2π. We chose cell phase advances of $\nu_{x\,c} = .270$ and $\nu_{y\,c} = .086$. Thus

$$\begin{aligned} 11\,\nu_{x\,c} &\approx 3 \qquad & 11(3\nu_{x\,c}) &\approx 9 \\ 11(\nu_{x\,c} + 2\nu_{y\,c}) &\approx 5 \qquad & 11(\nu_{x\,c} - 2\nu_{y\,c}) &\approx 1\ . \end{aligned} \tag{4.2}$$

While this choice of phase advance cancels the first order geometrics over an arc, it drives the octupole difference resonance, a second order geometric effect of sextupoles. Although we have not tried, we should be able to minimize the higher order geometric and higher order chromatic effects with additional sextupole families.

We have not attempted any optimization other than adjusting the cell phase advances as described above. The dynamic aperture is, for the most part, larger than the physical aperture. The results of tracking 1000 turns are plotted in Fig. 7. Note that the plot is distorted; the beam pipe is be round. The dynamic aperture will decrease when errors and realistic wiggler induced non-linear fields are included, but with more sophisticated chromatic correction schemes it should not present a problem.

5. TOLERANCES

5.1. Alignment

We need to calculate the effects of misalignments on both the dynamic aperture and the emittances. Errors in the machine decrease the dynamic aperture by causing tune shifts and higher order multipole fields on the closed orbit. In addition, errors will couple the horizontal and vertical planes and generate vertical dispersion, causing an increase in the vertical emittance. As mentioned in the previous section we have not yet attempted to optimize the chromatic correction scheme and the dynamic aperture; thus we only discuss the tolerances necessary to achieve the desired emittance ratio.

In an ideal uncoupled ring there is no vertical dispersion or linear coupling. Thus the synchrotron radiation opening angle, which is very small, determines the vertical emittance. In practice, this is not the case. First, vertical dipole errors and a non-zero vertical orbit in the quadrupole magnets will directly introduce some vertical dispersion. Second, a non-zero vertical orbit through the sextupole magnets, vertical sextupole misalignments, or rotational misalignments of the quadrupoles couple the horizontal and vertical planes. This coupling has two effects both of which increase the vertical emittance. It couples the horizontal dispersion to the vertical, causing an increase in the vertical, and it couples the x and y betatron motion so that energy is transferred between the two.

Assuming uncorrelated misalignments, the vertical emittance due to the dispersion generated by quadrupole rotations and sextupole misalignments is:

$$\begin{aligned}\gamma\epsilon_y &\approx \frac{2C_q\gamma^3}{J_y}\frac{\langle\eta_y^2\rangle}{\beta_y}\frac{\oint ds/\rho(s)^3}{\oint ds/\rho(s)^2}\\ \frac{\langle\eta_y^2\rangle}{\beta_y} &\approx \frac{1}{2\sin^2\pi\nu_y}\sum_{\{\text{quads}\}}(K_1L)^2\beta_y\Theta^2\\ \frac{\langle\eta_y^2\rangle}{\beta_y} &\approx \frac{1}{8\sin^2\pi\nu_y}\sum_{\{\text{sext}\}}(K_2L)^2\beta_y y_m^2\ ,\end{aligned}\tag{5.1}$$

where $C_q = 3.84\times10^{-13}$ m, Θ is the rotation angle, and y_m is the vertical sextupole misalignment. K_1L and K_2L are the integrated normalized quadrupole and sextupole strengths. Likewise, the increase in the vertical emittance due to linear coupling is:

$$\begin{aligned}\epsilon_y &\approx \epsilon_x\overline{\alpha}\frac{1-\cos\Psi_x\cos\Psi_y}{(\cos\Psi_x-\cos\Psi_y)^2}\sum_{\{\text{quads}\}}(K_1L)^2\beta_x\beta_y\Theta^2\\ \epsilon_y &\approx \epsilon_x\overline{\alpha}\frac{1-\cos\Psi_x\cos\Psi_y}{4(\cos\Psi_x-\cos\Psi_y)^2}\sum_{\{\text{sext}\}}(K_2L)^2\beta_x\beta_y y_m^2\ ,\end{aligned}\tag{5.2}$$

where $\Psi = 2\pi\nu$, and $\overline{\alpha} = (\alpha_x+\alpha_y)/\alpha_y$; $\alpha_{x,y}$ is the horizontal (vertical) damping rate. Note that both the formula for the dispersion and linear coupling have resonant denominators. The vertical dispersion grows as ν_y approaches an integer and the linear coupling contribution increases as ν_y approaches the linear sum or difference resonance. To minimize both these we chose the operating tunes $\nu_x = .37$ and $\nu_y = .27$.

It is harder to estimate the effects of the dipole errors since, in addition to generating vertical dispersion, dipole errors cause a vertical orbit which is correlated from point to point. We consider the limit of an orbit fully corrected with dipole correctors. We then approximate the orbit by assuming that it is correlated between correctors, but uncorrelated on either side of a corrector. In this case the vertical dispersion can be approximated as

$$\frac{\langle\eta_y^2\rangle}{\beta_y} \approx \frac{\langle y^2\rangle_{\text{res}}}{\beta_y}\left[1+\frac{1}{16\sin^2\pi\nu_y}\times\left(N_{\text{cell}}(4\pi\xi_{y\,\text{cell}})^2+N_{\text{ins}}(4\pi\xi_{y\,\text{ins}})^2\right)\right]\ ,\tag{5.3}$$

where $\langle y^2\rangle_{\text{res}}/\beta_y$ is the residual orbit after correction and $\xi_y = -1/4\pi\int\beta_y(K_1+K_2\eta_x)ds$ is the local vertical chromaticity of one cell or insertion region. Also, N_{corr} is the number of correctors being used and N_{ins} is the number of insertion regions. Note that this formula illustrates the advantage of local chromatic correction. The vertical dispersion due to a vertical closed orbit is a quadratic function of the *local* vertical chromaticity between correctors. This is one advantage of the FODO and TME[16] lattices over the Chasman-Green type structures. In the FODO or TME lattices, sextupoles can surround each quadrupole, whereas, in the Chasman-Green lattice all of chromatic correction is done at the center of each cell structure where the dispersion is non-zero. In our current design we have not yet attempted to minimize the chromaticity locally by correcting the arcs and insertions separately; all chromatic correction is done in the arcs.

Using the same approximation, that the orbit is uncorrelated across the correctors, the emittance due to the linear coupling is:

$$\epsilon_y = \frac{\epsilon_x\overline{\alpha}}{64}\frac{\langle y^2\rangle_{\text{res}}}{\beta_y}\sum_{\Delta\nu,\Delta\phi}\frac{N_{\text{corr}}}{\sin^2\pi\Delta\nu\sin^2\pi\Delta\phi_{\text{cell}}}\times\left(\sum_{i,j\in\text{cell}}(K_2L)_i(K_2L)_j\beta_{y\,i}\beta_{y_j}\sqrt{\beta_{x\,i}\beta_{x\,j}}\cos\Delta\phi_{i,j}\right)\ ,\tag{5.4}$$

where the first sum is over the two values of $\Delta\nu$, $\Delta\nu =$

$\nu_x \pm \nu_y$, and two values of $\Delta\phi$ for each value of $\Delta\nu$:

$$\Delta\phi_{i,j} = \begin{cases} \phi_{x\,i,j},\ \phi_{x\,i,j} + 2\phi_{y\,i,j}; & \Delta\nu = \nu_x + \nu_y \\ \phi_{x\,i,j},\ \phi_{x\,i,j} - 2\phi_{y\,i,j}; & \Delta\nu = \nu_x - \nu_y\ . \end{cases} \tag{5.5}$$

Here, $\phi_{i,j}$ is the phase advance between sextupole i and j in the cell and ϕ_{cell} is the cell phase advance. Notice that the expression becomes large when the tunes are close to the linear coupling resonances and when the cell phase advances are close to the sextupole coupling resonances.

Summing all of these contributions, we have

$$\gamma\epsilon_y \approx \Theta^2 8.9 \times 10^{-8} + y_m^2 10.5 \times 10^{-6} + \frac{\langle y^2\rangle_{\text{res}}}{\beta_y}1.8 \times 10^{-6}\ , \tag{5.6}$$

where Θ is the quadrupole rotational misalignment in milliradians and y_m and y_{res} are the sextupole misalignment and residual orbit in millimeters. Thus the vertical emittance depends strongly upon y_m and the residual orbit. We can specify tolerances by dividing most of the contribution between y_m and the closed orbit:

$$\Theta \leq 0.25\,\text{mrad}, \quad y_m \leq 30\,\mu\text{m}, \quad y_{\text{res}} \leq 100\,\mu\text{m}\ , \tag{5.7}$$

where $\overline{\beta}_y$ was assumed to be 2 m. Notice that random sextupole misalignments y_m are far more damaging than the residual orbit. In addition, with a vertical corrector in each cell, the residual orbit is strongly dependant on the BPM tolerances and only weakly dependant upon the magnitude of the dipole errors. Thus the BPM's must be aligned to a tolerance of $100\,\mu$m *minus* the BPM measurement sensitivity.

These results were verified with a computer program which, like PETROS, calculates the fully coupled emittances given a distribution of errors in the ring. Using 10 distributions of errors, the program consistently corrects the orbit due to $200\,\mu$m quadrupole misalignments to less than the $100\,\mu$m orbit tolerance. Furthermore, the average value of $\gamma\epsilon_y$ is very close to the results of these analytic formulas. Unfortunately, the rms of $\gamma\epsilon_y$ is quite large, about 70% of the average value, implying that we would need to tighten the tolerances to have confidence in the final emittance ratio.

Fortunately, we can correct much of the coupling. Linear coupling can be corrected with four orthogonal skew quadrupoles. Of course to correct the linear coupling, one has to measure the amount of coupling, and then separate the linear coupling from the effects of vertical dispersion. One option would be to use a number of profile monitors around the ring. The effects of the vertical dispersion could be subtracted off using the fact that the dispersion should oscillate at a harmonic next to the tune. Alternatively, we should be able to find the amplitude and phase of the linear coupling by measuring the phase and amplitude of the $\nu_x \pm \nu_y$ tune lines relative to the ν_x and ν_y lines.[27] We hope to test this technique on the SLC in the future.

We can also correct the vertical dispersion. Skew quads in regions of horizontal dispersion act much like dipole correctors when correcting a closed orbit. Just as when correcting a closed orbit, the first few correctors, skew quads in this case, do most of the correction. Obviously to correct both the linear coupling and the dispersion, we have to perform the corrections in an orthogonal manner.

5.2. Kickers

It is extremely important that the extraction kicker have very small jitter. Assuming linear optics, a one sigma jitter at the extraction septum becomes one sigma jitter at the IP. Actually, without BNS damping[28,29] the jitter would be magnified many times by transverse wakefields in the linac. But with weak BNS damping, the linear approximation is fairly accurate.

We would like to achieve a jitter tolerance of one tenth of the beam size $\sigma_{x,y}$ at the IP. This specifies a tolerance on the kicker. Assuming that the septum plate is 90° in phase downstream of the kicker,

$$\frac{\Delta\Theta}{\Theta} \leq \frac{\sigma_{\text{jit}}}{x_{\text{kick}}} \quad \text{where} \quad \sigma_{\text{jit}} \leq \frac{1}{10}\sigma_x\ , \tag{5.8}$$

where x_{kick} is the transverse displacement of the kicked beam at the septum. It is a sum of the distance between the closed orbit and the septum plate plus the septum thickness and some extra space for the extracted beam.

This tolerance can be written in a more transparent form:

$$\frac{\Delta\Theta}{\Theta} \leq \frac{1}{10}\frac{\sqrt{\gamma\epsilon_{\text{ext}}\beta_{x\,\text{sept}}}}{x_{\text{sept plate}} + 1\,\text{mm} + N_s\sqrt{\gamma\epsilon_{\text{inj}}\beta_{x\,\text{sept}}}}\ , \tag{5.9}$$

where $\gamma\epsilon_{\text{ext}}$ and $\gamma\epsilon_{\text{inj}}$ are injected and extracted beam emittances. N_s is the distance between the closed orbit and the septum plate in units of the injected beam size. To prevent particle loses, the septum plate must be many sigma from the stored beam just after *injection* when the beam is the largest; we assumed $N_s = 7$. The only other quantity in the tolerance is the septum plate thickness. Because a pulsed septum will introduce more jitter problems, we need to use a DC septum. The septum plate in a DC septum with strong fields cannot be made much thinner than 3 mm.[30] Assuming $\gamma\epsilon_{\text{inj}} = 3 \times 10^{-3}$ mrad and $\beta_x \approx 3$ m, the jitter tolerance on the kicker is

$$\frac{\Delta\Theta}{\Theta} \leq 3 \times 10^{-4}\ . \tag{5.10}$$

Notice that this tolerance is mainly determined by the ratio of the extracted beam emittance to the injected emittance. The only way to minimize the tolerance is to reduce N_s, increasing the particle loses due to scraping, or to reduce the injected emittance.

Such a tolerance will be difficult to achieve. One solution would be to use two kickers, separated by a phase advance of π, to cancel the jitter. One kicker would be placed before the septum and one located in the extraction line. Unfortunately, this approach requires that the two kickers track each other over the time needed to extract a batch, ~ 7 ns. Since the tolerance for this bunch to bunch tracking is equal to the jitter tolerance, getting the two kickers to track maybe as difficult a problem as having a single kicker to achieve the jitter tolerance. An alternate approach would be to use a current source with feedback instead of a thyratron. Unfortunately, with current technology, it is not apparent that such a system could provide the necessary current.[8] To conclude, we have not yet found a viable solution to the kicker problem and it requires further research.

6. SUMMARY

In this paper we present a design for a damping ring for a TeV linear collider. The ring is based upon a FODO lattice where the bending magnets contain a gradient to re-partition the damping. In addition, damping wigglers are used to lower the operating energy and to increase the energy spread. If the length of wiggler required is too much, we have solutions at higher energies that need less.

We demonstrate, using a very simple chromatic correction scheme, that the chromatically corrected ring has reasonable dynamic aperture. We also calculate the tolerances on the alignment and the vertical orbit necessary to achieve a 100:1 emittance ratio and then discuss methods of correcting the coupling. Finally, we calculate tolerances on the extraction kickers and find that they are very tight. Unfortunately this tolerance depends mainly upon the ratio of the injected beam emittance to the extracted emittance and it is not easy to decrease.

Finally, we note that we have more work in optimizing the injection/extraction insertion regions to loosen the requirements on the extraction kickers. We need to improve the chromatic correction scheme and we should calculate the effect of errors on the dynamic aperture. We also should also take detailed looks at designs based upon the TME lattice and a version of a FODO lattice without separate defocusing quadrupoles.

ACKNOWLEDGEMENTS

We would like to thank Bill Gabella for help with the preliminary design, Phil Morton and Martin Lee for many useful suggestions, and Martin Donald for discussions on chromatic correction.

REFERENCES

1. See references in these proceedings.
2. K. Thompson and R. D. Ruth, "Multibunch instabilities in Subsystems of 0.5 and 1.0 TeV Linear Colliders", *in these proceedings* and SLAC–PUB–4800 (1988).
3. L. Z. Rivkin, "Damping Ring for the SLC", Ph.D. Thesis, California Inst. Tech. (1986).
4. L. Z. Rivkin, *et. al.*, "Bunch Lengthening in the SLC Damping Ring", SLAC–PUB–4645 (1988).
5. R.B. Palmer, "Exotic Damping Ring Lattices", SLAC–PUB–4329 (1987).
6. J.D. Bjorken and S.K. Mtingwa,"Intrabeam Scattering", *Particle Accelerators*, **13**, 115 (1983).
7. Using the formalism of Bjorken and Mtingwa, Pisin Chen estimated the effect of intrabeam scattering on the vertical emittance and found it negligible.
8. F. Bulos, private communication.
9. M. Sands, "The Physics of Electron Storage Rings", SLAC–121 (1970).
10. J. M. Wang and C. Pellegrini, *Proceedings of the 11th Int. Conf. on High Energy Acc.*, Geneva, Switzerland (1980), p. 554.
11. *Proceedings of the ICFA Workshop on Low Emittance e^--e^+ Beams*, BNL, March 20-25 1987.
12. S. Kheifets, "Bunch Compression for the TLC", *in these proceedings* and SLAC–PUB–4802 (1988).
13. K.W. Robinson, *Phys Rev.*, **111**, 373 (1958).
14. A. Hofmann, "Emittance Reduction in PEP with a Robinson Wiggler", SSRL–ADC–NOTE–40 (1986).
15. G. Vignola, "The Use of Gradient Magnets in Low Emittance Storage Rings", *Nucl. Instr. and Meth.*, **A246**, 12 (1986).
16. A. van Steenbergen, "Collider Damping Ring, Theoretical Minimum Emittance Structures", *Proceedings of the ICFA Workshop on Low Emittance e^--e^+ Beams*, BNL (1987), p. 60.
17. H. Wiedemann, "Design of Low Emittance Storage Rings", *Nucl. Instr. and Meth.*, **A246**, 4 (1986).
18. J. Bisognano *et. al.*, "Feasibility Study of a Storage Ring for a High-Power XUV Free-Electron Laser", *Particle Accelerators*, **18**, 223 (1986).
19. A. Jackson, "A Comparison of the Chasman-Green and Triple Bend Achromat Lattices", LBL–21279 (1986).
20. K. Halbach, *J. Appl. Phys.*, **57**, 3605 (1985).
21. C. Bazin, *et. al.*, "A Five-Pole Superconducting Wiggler for the DCI Positron Ring at LURE", *Nucl. Instr. and Meth.*, **A266**, 132 (1988).
22. H. Wiedemann, "Emittance in a FODO Lattice", PEP-303 (1979).
23. M. Zisman *et al.*,"ZAP User's Manual", LBL–21270 (1986).
24. J.E. Spencer, "Permanent Magnet Sextupole Protocol and Tolerances for the Damping Rings", SLAC–CN–309 (1985).
25. Klaus Halbach, private communication.
26. T. O. Raubenheimer and R. D. Ruth, "Superconvergent Tracking", *Particle Accelerators*, **23**, 197 (1988).
27. J. Bengtsson, "Non-Linear Transverse Dynamics for Storage Rings", CERN 88-05 (1988).
28. V. Balakin, A. Novokhatsky, V. Smirnov, *Proceedings of the 12th Int. Conf. on High Energy Accelerators*, Fermilab (1983), p. 119.
29. K. Bane, *IEEE Trans. Nucl. Sci.*, **NS-32**, 2389 (1985).
30. G. Fisher, private communication.